

Supplementary Information

Experimental Methods

HTPV devices were modeled using a photon accounting method. The band gap of the organic top cell was allowed to vary from 1.1-3.5 eV. The absorbance was assumed to be step-shaped, with zero absorbance below the band gap energy and constant absorbance for all energies above. The internal quantum efficiency was assumed to be 90%, and spectrally independent, which is characteristic of current top performing BHJ devices.^{1,2} The exact amount of parasitic absorption in an HTPV device will depend on the specific layers used. We have assumed that 10% of the incident light at all wavelengths is parasitically absorbed or reflected before it is incident on the top cell active layer. This absorption could be due to the top electrode absorption, or due to reflections present in the HTPV stack that are not present in the inorganic cell by itself, though it is beyond the scope of this work to account for them exactly. In 4-terminal devices, we assumed an additional 10% of the light was lost after leaving the top cell but before reaching the bottom cell. This parasitic absorption means that the efficiencies of HTPV devices (Figure 3) do not converge with those of the inorganic cells by themselves as the top cell band gap becomes very large. The Voc of the organic top cell was taken as 0.6 eV less than the band gap of the absorber divided by the electron charge, which corresponds to an empirical upper limit scaling often found for polymer BHJs,³ and was assumed to be independent of the bottom cell or tandem wiring configuration. The fill factor of the organic top cell was assumed to be 0.70 in all devices, which corresponds to that

achieved by the current top performing BHJs,^{1,4} and to be independent of the polymer band gap.

The J_{sc} of the top cell was calculated by spectrally integrating its quantum efficiency multiplied by the AM1.5G spectrum according to:

$$J_{sc} = \int \eta(\lambda) A(\lambda) \phi(\lambda) d\lambda \quad (1)$$

where A is the absorption of the top cell absorber and ϕ is the flux of photons in the AM1.5G spectrum less the assumed parasitic absorption. The J_{sc} of the inorganic solar cell was calculated by integrating the external quantum efficiency (EQE) of the inorganic cell multiplied by the spectrum of light transmitted through the organic top cell, according to Equation 1. We assumed that the V_{oc} and FF of the inorganic bottom cells are the same in the HTPV cells as they are in the independent inorganic devices. In actuality the V_{oc}, and to a lesser extent the FF, of the inorganic bottom cell is slightly reduced by having the top cell filter out the high energy photons, however this effect is small (~2-3% relative loss as determined by PC1D⁵) and only weakly dependent on the top cell band gap when the top cell band gap is near optimal. EQE spectra for inorganic bottom cells were obtained from a variety of sources, and are shown in Supplementary Figures 1 and 2. The EQE spectra, V_{oc} and FF of silicon bottom cells were simulated using the device simulator, PC1D⁵ assuming 0.3 μm n-type emitter ($N_D = 1 \times 10^{19} \text{ cm}^{-3}$) and a 300 μm p-type base ($N_A = 1 \times 10^{16} \text{ cm}^{-3}$), which is a standard device architecture.⁶ Light was assumed to be incident on the emitter side. There was a 0.1 Ohm series resistance component at

the emitter, corresponding to the finite conductance of the silver fingers. Zero shading was assumed for the silver fingers, though in actual silicon solar cells of this architecture several percent of the light will be lost. In the high-quality material, the Shockley-Reed-Hall (SRH) recombination lifetime was assumed to be 1 ms in both the emitter and the base, which is typical of high quality and purity material.⁷ PC1D takes into account Auger recombination separately based on the doping, which will further reduce the minority carrier lifetime in the emitter from this nominal value. In the low quality material, the SRH recombination lifetime was assumed to be 1 μ s, which corresponds to the lower echelon of multi-crystalline wafers.⁸ In the unpassivated devices, the surface recombination velocity at the top surface (emitter side) was taken to be 2×10^5 cm/s, which corresponds to bare silicon.⁹ In the cells with good passivation the surface recombination velocity at the top surface was taken to be 250 cm/s, which corresponds to a decent quality n-Si/ SiO₂ interface, but is a little higher than that of an n-type emitter passivated by PECVD deposited SiN_x (~ 60 cm/s).¹⁰ In all scenarios, the surface recombination velocity at the rear surface (base contact) was taken to be 1×10^6 cm/s, which corresponds to a Si-metal interface,⁹ and a back surface field was not included.

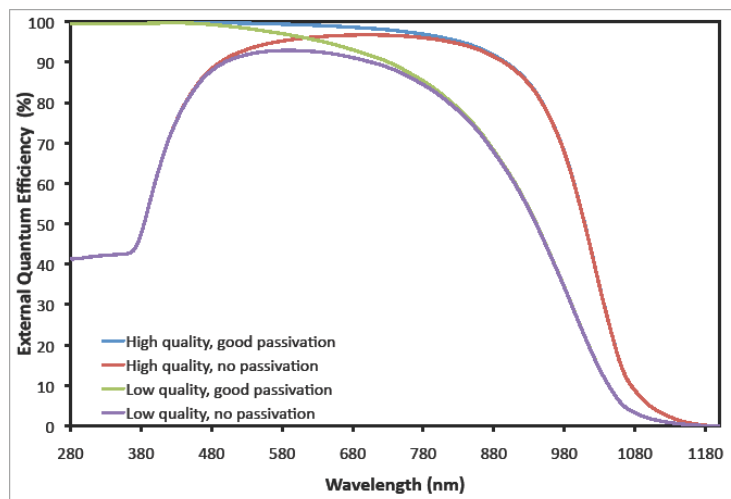
For the CIGS bottom cells considered here, EQE spectra (Supplementary Figure 2) Voc's and FF's were taken directly from the literature. The high efficiency CIGS cell was made at NREL by vacuum co-evaporation¹¹ and the more moderate efficiency cell was a commercially produced device from HelioVolt,¹² made by a proprietary reactive transfer process (FASSTTM). Because external quantum efficiency curves

were used, they already reflect the parasitic absorption that is inherent to the CdS window layer and transparent conducting oxide electrodes. These parasitic absorptions will be present to a similar degree in an HTPV device made from these bottom cells, but we have still assumed an additional 10% broad spectrum parasitic absorption in the layers associated with the organic top cell. The J_{sc} of the HelioVolt CIGS cell was obtained by integrating its EQE spectrum multiplied by the AM1.5G spectrum, which gave a J_{sc} that was slightly higher than the J_{sc} reported alongside the V_{oc} and FF of that device. As a result, the PCE of the HelioVolt cell by itself was assumed to be 15.1% instead of the reported 14%.¹²

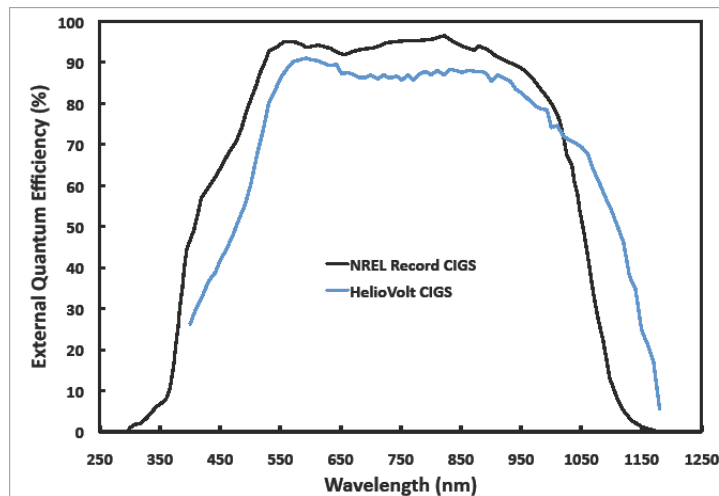
In the current matched devices, the current of the tandem cell was taken to be the lesser of the J_{sc} 's from the two subcells, which has been shown to be a good approximation for the current of a series connected tandem.¹³ The fill factor of the tandem devices was taken to be the mean of the two independent subcell fill factors. This has been shown to be a slight overestimate of the tandem fill factor when the two subcells have significantly different fill factors. However, for the cases considered here where the organic fill factor is at most 16% less than the inorganic fill factor, this approximation overestimates the tandem fill factor by less than 3%.¹³ The V_{oc} of the tandem devices was taken as the sum of the two independent subcell V_{oc} 's.¹³ In the independently operated devices (4-terminal), the power output of the HTPV device was assumed to be the sum of the powers of the subcells, with no current or voltage matching constraints.

Supplementary Table 1: Figures of merit for the inorganic bottom cells considered here operating by themselves.

Bottom Cell Type	Scenario	Voc	FF	Stand Alone Efficiency
Silicon	High quality, good passivation	621 mV	0.83	19.4%
	High quality, no passivation	604 mV	0.82	17.5%
	Low quality, good passivation	574 mV	0.81	15.4%
	Low quality, no passivation	569 mV	0.81	14.2%
CIGS	HelioVolt Cell ¹²	631 mV	0.72	15.1%
	NREL Cell ¹¹	690 mV	0.81	19.9%



Supplementary Figure 1: EQE spectra of the silicon bottom cells considered here, as determined by PC1D.



Supplementary Figure 2: EQE spectra of the CIGS bottom cells considered here.

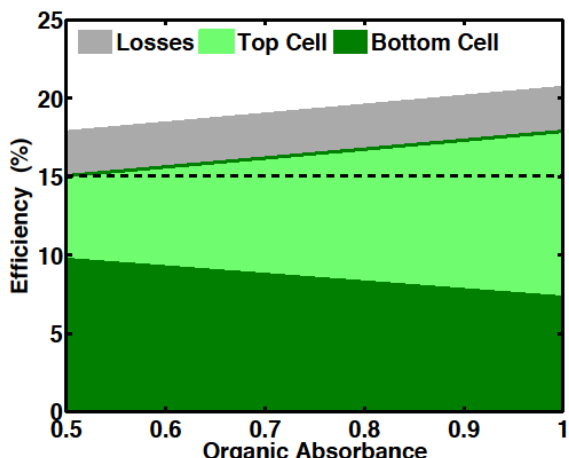
Figures of Merit for Modeled Hybrid Tandems

Supplementary Table 2: Figures of merit for current matched (2-terminal) hybrid tandem cells. The organic top cell is assumed to have the optimal band gap for each device configuration and to absorb all of the above band gap light (after subtracting parasitic absorption).

Bottom Cell Type	Scenario	Jsc (mA/cm ²)	Voc (V)	FF	Efficiency
Silicon	High quality, good passivation	16.1	1.81	0.77	22.3%
	High quality, no passivation	16.0	1.79	0.76	21.8%
	Low quality, good passivation	14.2	1.84	0.76	19.8%
	Low quality, no passivation	14.2	1.85	0.76	19.8%
CIGS	HelioVolt Cell	16.9	1.78	0.71	21.4%
	NREL Cell	16.9	1.85	0.76	23.5%

Supplementary Table 3: Figures of merit for independently operated (4-terminal) hybrid tandem cells. The organic top cell is assumed to have the optimal band gap for each device configuration and to absorb all of the above band gap light (after subtracting parasitic absorption).

Bottom Cell Type	Scenario	Bottom Cell				Top Cell				Tandem Efficiency
		Jsc (mA/cm ²)	Voc (mV)	FF	Efficiency	Jsc (mA/cm ²)	Voc (mV)	FF	Efficiency	
Silicon	High quality, good passivation	18.4	0.621	0.83	9.5%	12.2	1.38	0.70	11.8%	21.3%
	High quality, no passivation	17.3	0.604	0.82	8.6%	13.2	1.33	0.70	12.3%	20.8%
	Low quality, good passivation	13.5	0.574	0.81	6.3%	13.6	1.31	0.70	12.5%	18.7%
	Low quality, no passivation	13.4	0.569	0.81	6.2%	13.6	1.31	0.70	12.5%	18.6%
CIGS	HelioVolt Cell	16.6	0.631	0.72	7.5%	15.5	1.22	0.70	13.2%	20.8%
	NREL Cell	19.5	0.690	0.81	10.9%	12.2	1.38	0.70	11.8%	22.7%



Supplementary Figure 3: PCE of HTPV devices with a HelioVolt CIGS bottom cell as a function of absorbance of the organic active layer, assuming that the top cell Voc is fixed at 945 mV and the organic band gap is 1.8 eV. The grey portion shows the assumed losses due to parasitic absorption.

Estimate of Costs for HTPV modules

Under the assumptions in the present work, the addition of an organic top cell can improve the efficiency of a HelioVolt CIGS cell from 15.1% to 21.4% (a 42% relative increase) in a 2-terminal configuration. The addition of an organic top cell then, will reduce the cost of the CIGS cell if it increases the area cost of the CIGS cell by less than 42%. Roadmaps for the development of CIGS technology call for the reduction of costs to $\sim \$0.55 /W_p$ and module efficiencies of $\sim 15\%$.¹⁴ At $\$0.55 /W_p$ and 15.1% PCE, the projected area cost of a CIGS cell by itself is $83 \text{ \$/m}^2$. Then adding an organic top needs to cost less than $35 \text{ \$/m}^2$ if it is to reduce the overall cost of the CIGS cell. Using more current estimates¹⁵ (from 2011) of the cost and efficiencies of CIGS modules ($\$1.13 /W_p$ with $\sim 12\%$ modules),¹⁴ the area cost of the CIGS cell by itself is $136 \text{ \$/m}^2$ so the organic top cell must cost less than $57 \text{ \$/m}^2$.

A rigorous breakdown of the costs of producing polymer photovoltaics has recently been performed by Azzopardi *et al.*¹⁶, and we use this here as a rough estimate for the cost of adding an organic top cell (Supplementary Table 4). Azzopardi *et al.* estimate materials costs from current market prices for the raw materials as well as any additional materials required during processing of the layers. From these numbers we arrive at an estimate of $\sim 17 \text{ \$/m}^2$ for the materials costs of adding an organic top cell, which is well within the margin for cost reduction determined by the improvement in efficiency. This includes the active material as well as electron and hole collecting layers (ZnO and PEDOT: PSS, respectively), but does not include any additional transparent conducting oxide or electrodes. In a 2-terminal tandem, there are only two electrodes, which in principle are similar to those in a single junction inorganic cell, so that the cost of the electrodes is already carried in the estimate of the CIGS module cost. Since the top cell layers may be deposited by inexpensive, low-temperature techniques, such as spray-coating, slot-coating or ink-jet printing, the materials costs of the organic top cell dominates its processing costs (estimated¹⁶ to be $< 0.5 \text{ \$/m}^2$). Given a top cell cost $\sim 17 \text{ \$/m}^2$, the cost of a 15.1% CIGS cell, can be reduced by 15% from $\$0.55 /W_p$ to $\$0.47 /W_p$ when an organic top cell is added to make an HTPV device. Using the more current cost estimates for CIGS cells ($136 \text{ \$/m}^2$) and assuming that the top cell improves the efficiency of the CIGS by 42%, then the organic top cell can reduce the module cost by $\sim 21\%$. Thus we estimate the range of potential cost reductions for CIGS technology as $\sim 15\text{-}20\%$ with the addition of an organic top cell in a 2-terminal configuration. Furthermore, the large increase in efficiency of the cells means that fewer modules need to be

installed to obtain equivalent power from a photovoltaics system. This leads to a reduction in the installation cost of the panels of up to 30% for the increases in efficiency considered here, assuming that the installation cost per unit area is unchanged.

Supplementary Table 4: Summary of estimated materials costs for the organic top cell.¹⁶ ZnO is the electron collecting layer, PEDOT is the hole collecting layer and P3HT/ PCBM is the organic absorber (active layer).

	Material Cost (\$/m²)
ZnO	0.09
P3HT/ PCBM	11.15
PEDOT	5.73
Total	16.97

References

1. Y. Liang, Z. Xu, J. Xia, S.-T. Tsai, Y. Wu, G. Li, C. Ray, and L. Yu, *Advanced Materials*, 2010, **22**, E135–E138.
2. S. H. Park, A. Roy, S. Beaupre, S. Cho, N. Coates, J. S. Moon, D. Moses, M. Leclerc, K. Lee, and A. J. Heeger, *Nature Photonics*, 2009, **3**, 297–302.
3. D. Veldman, S. C. J. Meskers, and R. A. J. Janssen, *Adv. Funct. Mater.*, 2009, **19**, 1939–1948.
4. C. Piliego, T. W. Holcombe, J. D. Douglas, C. H. Woo, P. M. Beaujuge, and J. M. J. Frechet, *J. Am. Chem. Soc.*, 2010, **132**, 7595–7597.
5. D. A. Clugston and P. A. Basore, *Conference Record of the Twenty-Sixth IEEE Photovoltaic Specialists Conference*, 1997, 207–210.
6. J. Nelson, *The physics of solar cells*, World Scientific Pub Co Inc, 2003.
7. J. Schmidt and A. G. Aberle, *Journal of Applied Physics*, 1997, **81**, 6186.
8. A. Cuevas, M. Stocks, D. McDonald, M. Kerr, and C. Samundsett, *IEEE Transactions on Electron Devices*, 1999, **46**, 2026–2034.
9. A. Cuevas, P. A. Basore, G. Giroult-Matlakowski, and C. Dubois, *Journal of Applied Physics*, 1996, **80**, 3370–3375.
10. A. G. Aberle, *Prog. Photovolt: Res. Appl.*, 2000, **8**, 473–487.
11. I. Repins, M. A. Contreras, B. Egaas, C. DeHart, J. Scharf, C. L. Perkins, B. To, and R. Noufi, *Prog. Photovolt: Res. Appl.*, 2008, **16**, 235–239.
12. L. Eldada, *SPIE Photonics West*, 2011.
13. A. Hadipour, B. de Boer, and P. W. M. Blom, *Organic Electronics*, 2008, **9**, 617–624.
14. N. G. Dhere, *Sol Energ Mat Sol C*, 2011, **95**, 277–280.

15. A. Goodrich, *37th IEEE Photovoltaic Specialists Conference*, 2011.
16. B. Azzopardi, C. J. M. Emmott, A. Urbina, F. C. Krebs, J. Mutale, and J. Nelson, *Energy & Environmental Science*, 2011, **4**, 3741.